Nuclear Instruments and Methods in Physics Research B 267 (2009) 2827–2831

Contents lists available at ScienceDirect

Nuclear Instruments and Methods in Physics Research B

journal homepage: www.elsevier.com/locate/nimb

Ion irradiation induced nanocrystal formation in amorphous $Zr_{55}Cu_{30}Al_{10}Ni_5$ alloy

Jesse Carter [a], E.G. Fu [b], Michael Martin [a], Guoqiang Xie [c], X. Zhang [b], Y.Q. Wang [d], D. Wijesundera [e], X.M. Wang [e], Wei-Kan Chu [e], Sean M. McDeavitt [a], Lin Shao [a,*]

[a] Department of Nuclear Engineering, Texas A&M University, College Station, TX 77843, United States
[b] Department of Mechanical Engineering, Texas A&M University, College Station, TX 77843, United States
[c] Institute for Materials Research, Tohoku University, Sendai 980-8577, Japan
[d] Los Alamos National Laboratory, Los Alamos, NM 87545, United States
[e] Texas Center for Superconductivity and Department of Physics, University of Houston, Houston, TX 77204, United States

ARTICLE INFO

Article history:
Received 8 April 2009
Received in revised form 16 May 2009
Available online 6 June 2009

PACS:
61.66.Dk
61.80.−x
61.82.Bg

Keywords:
Metallic glass
Ion irradiation
Crystallization

ABSTRACT

Ion irradiation can be used to induce partial crystallization in metallic glasses to improve their surface properties. We investigated the microstructural changes in ribbon $Zr_{55}Cu_{30}Al_{10}Ni_5$ metallic glass after 1 MeV Cu-ion irradiation at room temperature, to a fluence of 1.0×10^{16} cm^{-2}. In contrast to a recent report by others that there was no irradiation induced crystallization in the same alloy [S. Nagata, S. Higashi, B. Tsuchiya, K. Toh, T. Shikama, K. Takahiro, K. Ozaki, K. Kawatusra, S. Yamamoto, A. Inouye, Nucl. Instr. and Meth. B 257 (2007) 420], we have observed nanocrystals in the as-irradiated samples. Two groups of nanocrystals, one with diameters of 5–10 nm and another with diameters of 50–100 nm are observed by using high resolution transmission electron microscopy. Experimentally measured planar spacings (*d*-values) agree with the expectations for $Cu_{10}Zr_7$, $NiZr_2$ and $CuZr_2$ phases. We further discussed the possibility to form a substitutional intermetallic $(Ni_xCu_{1-x})Zr_2$ phase.

1. Introduction

Due to the absence of long range atomic order, metallic glasses (MGs) have attracted tremendous attention because of their unique mechanical, thermal and chemical properties [1–7]. However, MGs will develop ordered structures if enough energy is supplied. Numerous studies have shown that nanocrystals can be formed under annealing [8], deformation [9], bending [10], nanoindentation [11] and ion or electron irradiation [12–16]. Although the specific mechanisms that induce partial crystallization are different in each of these cases, the general crystallization phenomena are typically associated with enhanced atomic mobility. Inducing nanocrystalization in MGs is of scientific and technological interest since the induced nanocrystals will interact with shear sliding and inhibit shear band propagation during deformation [17–19]. This has the effect of making the brittle MGs more ductile and thus more suitable for broader applications.

The metallic glass alloy $Zr_{55}Cu_{30}Al_{10}Ni_5$ has been well studied since it exhibits excellent glass forming ability with a wide supercooled liquid region [20–26]. It belongs to a group of MGs that have the capability to retain their amorphous structure even at a low cooling rate. Thus, this material is available for fabrication as a large-scale amorphous MG suitable for structural applications.

A number of studies have been carried out to understand the stability of this $Zr_{55}Cu_{30}Al_{10}Ni_5$ alloy. Under thermal annealing at temperatures around 750 K, crystalline decomposition products such as $NiZr_2$, $CuZr_2$ and $Cu_{10}Zr_7$ phases have been observed [22]. Due to its wide supercooled liquid region, amorphous $Zr_{55}Cu_{30}Al_{10}Ni_5$ has been reported to be stable under electron irradiation [27]. However, its stability under ion irradiation is controversial. Recently, ion irradiation effects in $Zr_{55}Cu_{30}Al_{10}Ni_5$ were studied by two groups [28,29]. In the study by Iqbal et al., it was reported that Ar ion irradiation did induce crystalline $CuZr_2$ phase formation [28]. In another study by Nagata et al., precipitation of crystalline phases was not observed after irradiation with various ions in $Zr_{55}Cu_{30}Al_{10}Ni_5$ [29]. The very different conclusions of the effects of ion irradiation in MG show the need for further studies.

In the present study, we have investigated the microstructural changes in $Zr_{55}Cu_{30}Al_{10}Ni_5$ glass after irradiation with 1 MeV Cu ions at room temperature, to a fluence of 1×10^{16} cm^{-2}. The selection of Cu ions avoids the complexity caused by impurity induced chemical effects. The fluence was selected to create considerable displacements, but causing negligible composition changes.

* Corresponding author. Tel.: +1 9798454107; fax: +1 9798456443.
E-mail address: lshao@mailaps.org (L. Shao).

0168-583X/$ - see front matter © 2009 Elsevier B.V. All rights reserved.
doi:10.1016/j.nimb.2009.05.068

2. Experimental procedure

The $Zr_{55}Cu_{30}Al_{10}Ni_5$ metallic glass ribbon samples used in this study were prepared by rapid solidification and are approximately 20 μm thick and 1.5 mm wide. The 1 MeV Cu-ion irradiation was performed to a fluence of 1×10^{16} cm^{-2} by using a NEC 1.7 MeV tandem accelerator. The beam flux was 6.3×10^{10} ion s^{-1} cm^{-2} and the sample's temperature during ion irradiation was measured to be less than 50 °C. No annealing was performed after irradiation. The samples were characterized before and after irradiation by X-ray diffraction (XRD), transmission electron microscopy (TEM), and high resolution transmission electron microscopy (HRTEM). XRD analysis used a Bruker-AXS D8 VARIO high resolution X-ray diffractometer. The TEM and HRTEM were performed by using a 200 kV JEOL 2010 microscope equipped with a Gatan SC1000 ORIUS CCD camera. For TEM specimen preparation, 2 keV Ar ion milling with the sample cooled by a liquid nitrogen cooling system was performed on a Fischione 1010 ion mill. The specimens were slowly rotated during thinning to avoid inhomogeneous etching. Furthermore, each TEM image was taken with minimal electron irradiation. Our recent studies have shown that the above specimen preparation procedure is necessary to avoid ion milling induced microstructural changes [30].

3. Results and discussion

Fig. 1 shows a bright-field TEM micrograph and corresponding selected area diffraction (SAD) pattern from the as-spun $Zr_{55}Cu_{30}Al_{10}Ni_5$ ribbon. No trace of crystalline phases and precipitations are found. The SAD pattern has wide halo rings without spots, which is a typical amorphous characteristic. Differential scanning calorimetry measurements (not shown here) on the as-spun sample also reveal a typical annealing behavior of MG with glass transition at 697 K and first-step crystallization at 762 K.

Fig. 2 shows XRD spectra of the as-spun and irradiated ribbon $Zr_{55}Cu_{30}Al_{10}Ni_5$ glasses. The as-spun sample shows a broad peak, which confirms its glassy state. After ion irradiation, this broad peak becomes narrower and the peak shifts and splits as it becomes more defined, which suggests the development of a more ordered structure. The XRD spectrum from the irradiated sample clearly shows sharp diffraction peaks superimposed on the broad amorphous peak. This suggests the existence of crystalline phases. As marked in Fig. 2, the sharpest peaks can be assigned to $Cu_{10}Zr_7$ and $NiZr_2$ phases. Further determination of crystalline phases by using TEM will be discussed later.

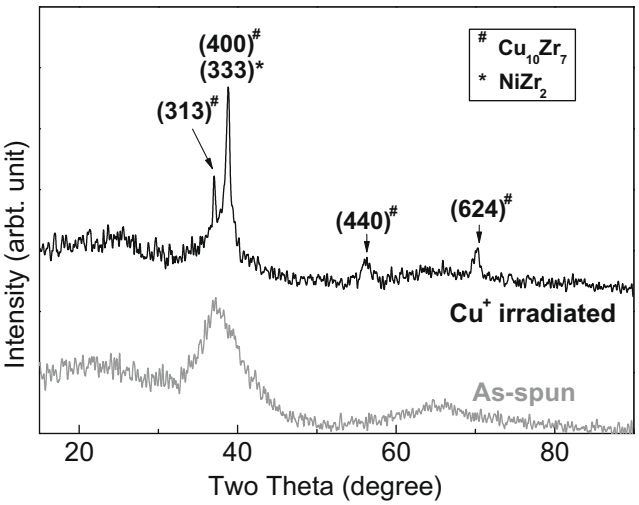

Fig. 2. XRD patterns of as-spun and Cu-ion irradiated $Zr_{55}Cu_{30}Al_{10}Ni_5$ glass. Diffraction peaks from crystalline $Cu_{10}Zr_7$ and $NiZr_2$ phases are marked.

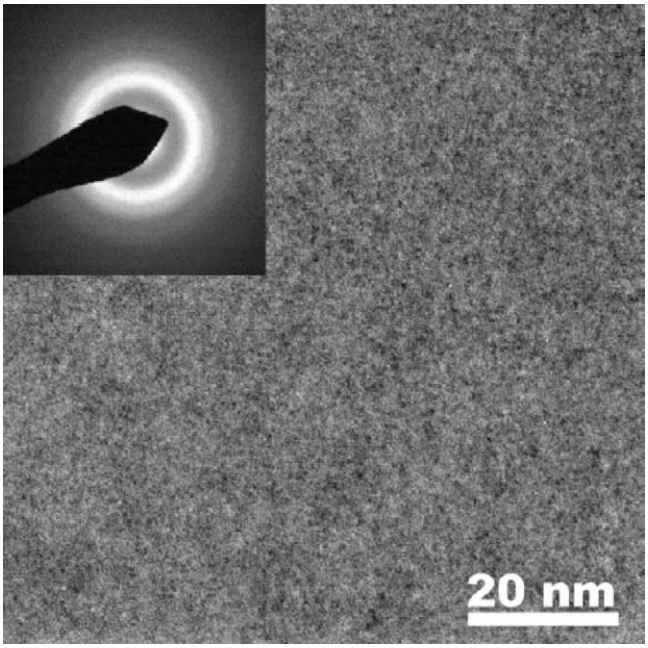

Fig. 1. Bright-field TEM micrograph of as-spun $Zr_{55}Cu_{30}Al_{10}Ni_5$ glass and the corresponding SAD pattern.

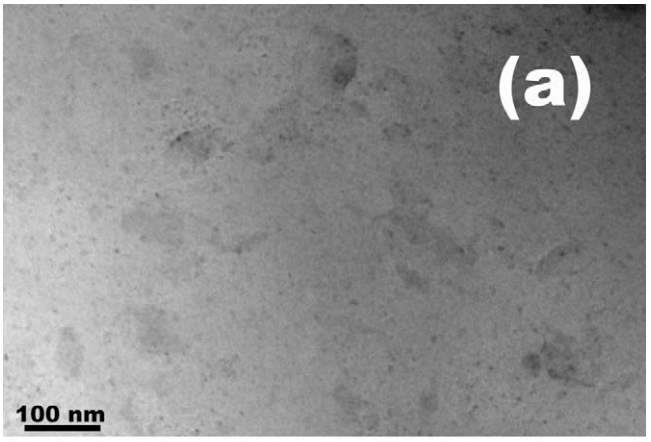

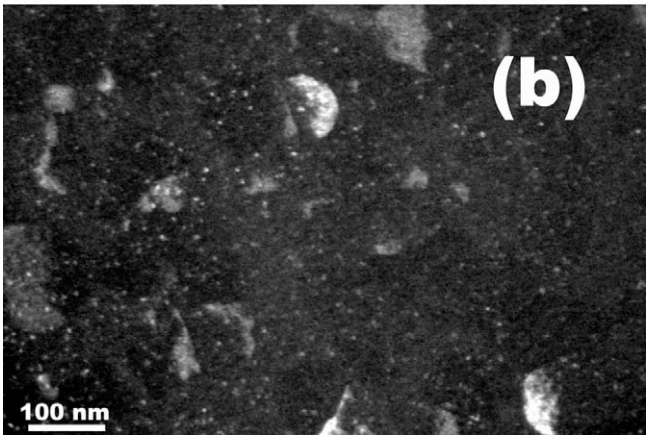

Fig. 3. (a) Bright-field TEM micrograph and (b) dark-field TEM micrograph of the Cu-ion-irradiated $Zr_{55}Cu_{30}Al_{10}Ni_5$ glass.

Fig. 3(a) and (b) shows bright field and dark-field TEM images, respectively, from the sample after 1 MeV Cu-ion irradiation (fluence = 1×10^{16} cm^{-2}). The prominent features observed in these images represent a dispersion of small crystalline particles, which is a dramatic contrast to the featureless amorphous alloy shown in Fig. 1. In Fig. 3(a), small particles with a typical size of 5–10 nm and large particles with a typical size of 50–100 nm are observed. In the corresponding dark-field TEM image in Fig. 3(b), both small and large particles show crystallinity.

Fig. 4 displays a high resolution TEM image from the irradiated sample, revealing the nanocrystal formations in the glassy matrix in greater detail. It is important to note that no preferential crystalline orientations are observed. The inset shows an inverse fast Fourier transform (FFT) of the image from the region marked by dash lines. The ordered crystalline structure is clearly visible. Fig. 5 shows an enlarged selected area diffraction (SAD) pattern for the TEM image obtained from the irradiated sample. Multiple interplanar distances were calculated based on diffraction points observed in this SAD pattern and these spacings were compared with a diffraction database [31]. The calculation considered instrument errors (~6%) by using a pure single crystal Si (1 0 0) sample for calibration.

Table 1 summarizes the experimentally obtained lattice spacings (d-values) compared with corresponding d-values and planar indices that would be present if $Cu_{10}Zr_7$, $NiZr_2$ or $CuZr_2$ had formed. The experimental d-spacing of 2.636 Å can be exclusively assigned to the (2 0 4) plane from $Cu_{10}Zr_7$. Thus, the observed crystalline phases in Figs. 3 and 4 should include $Cu_{10}Zr_7$. This observation is strengthened by the calculated d-values at 2.890 Å and 1.280 Å which correspond more closely with the $Cu_{10}Zr_7$ phase than the $NiZr_2$ or $CuZr_2$, respectively. The experimental d-values between 1.411 Å and 1.759 Å correspond closely with database d-values for all three compounds: $Cu_{10}Zr_7$, $NiZr_2$ and $CuZr_2$ with no clear distinction in favor of one phase over the other. The experimental d-values between 0.948 Å and 1.205 Å as well as 2.489 Å may be related to lattice planes from $NiZr_2$ and $CuZr_2$ with no clear distinction in favor of one phase over the other. Therefore, we can declare with certainty that the $Cu_{10}Zr_7$ intermetallic has formed within the irradiated metallic glass samples. Further, the additional d-spacings that could only arise from the presence of $NiZr_2$ or $CuZr_2$ indicate that the observed crystals are a mixture of $Cu_{10}Zr_7$ with $NiZr_2$ or $CuZr_2$ or both phases.

Stability studies on electron irradiated Zr-based MG have shown that $CuZr_2$ is a common stable decomposition product in Zr–Cu metallic glasses [32]. Further more, studies on the behavior

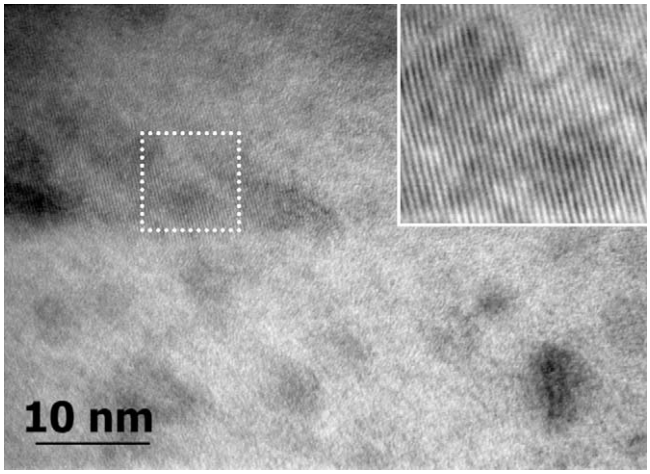

Fig. 4. High resolution TEM micrograph of Cu-ion-irradiated $Zr_{55}Cu_{30}Al_{10}Ni_5$ glass.

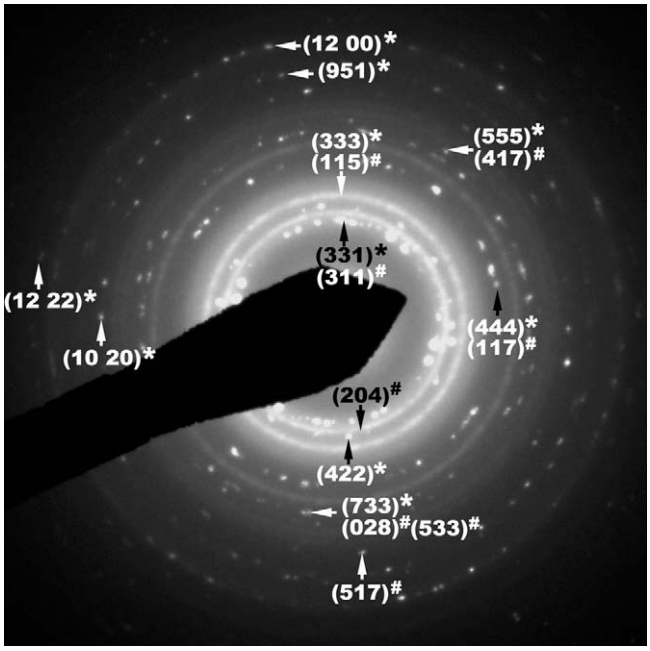

Fig. 5. The SAD pattern of Cu-ion-irradiated $Zr_{55}Cu_{30}Al_{10}Ni_5$ glass. The indexing indicates the co-existence of $Cu_{10}Zr_7$ (#) and $NiZr_2$ (*) phases.

Table 1
Comparison of d-spacing (in Å) from the present study and from database [31].

Experimental data: d-spacing from the present study	$Cu_{10}Zr_7$ standard d-spacing/ orientation (orthorhombic)	$NiZr_2$ standard d-spacing/ orientation (cubic)	$CuZr_2$ standard d-spacing/ orientation (tetragonal)
2.890	2.880/(311)	2.812/(331)	
2.636	2.621/(204)		
2.489		2.503/(422)	2.429/(103)
2.326	2.366/(115)	2.360/(333)	
1.759	1.746/(117)	1.767/(444)	1.761/(114)
1.496	1.499/(028), (533)	1.498/(733)	1.441/(116)
1.411	1.416/(417)	1.420/(555)	1.429/(211)
1.280	1.287/(517)		1.219/(206)
1.205		1.203/(1020)	1.191/(118)
1.179		1.187/(951)	1.158/(109)
1.039		1.021/(1200)	1.030/(303)
0.948		0.995/(1222)	0.941/(219)

of thermally annealed $Zr_{52}Ti_5Cu_{18}Ni_{15}Al_{10}$ MG have observed the formation of a $NiZr_2$ phase [33]. The observations noted above of crystalline planes from either $NiZr_2$ or $CuZr_2$ phases are consistent with these early studies. In fact, the similarity between Ni and Cu in electronegativity (1.8 and 1.9) and atomic radius (0.125 nm and 0.128 nm) coupled with the similar stoichiometry of $NiZr_2$ and $CuZr_2$ and tetragonal structures may imply the mutual solubility of $NiZr_2$ and $CuZr_2$. This would imply that a single phase structure with a structure similar to $(Ni_x,Cu_{1-x})Zr_2$ may have formed. This type of substitutional intermetallic structure is commonly observed in Fe–Cr–Ni–Zr alloy systems, where $Zr(Fe_x,Cr_y,Ni_z)_2$ and $(Fe_x,Cr_y,Ni_z)Zr_2$ ($x + y + z = 1$) intermetallics have been characterized [34,35].

It is interesting to note that the monoclinic CuZr phase was not observed here, even though it has the simplest CsCl-type structure. This is because CuZr is thermodynamically unstable at room temperature [36]. Stable CuZr phases do form at a high temperature (>985 K) [37] and if the cooling rate is high enough, they may avoid decomposition and exist at low temperatures. Otherwise, they are known to decompose into $Cu_{10}Zr_7$ and $CuZr_2$ phases [38]. The $Cu_{10}Zr_7$ has a complex

unit cell containing 68 atoms [39]. Although its formation requires highly correlated atomic movements, the required kinetics for nucleation are apparently favorable since this phase was frequently observed in thermal annealing of the Cu–Zr system [40].

All of these observations, taken together, point to the formation of two crystalline intermetallic phases within the irradiated metallic glass structure: $Cu_{10}Zr_7$ and $(Ni_x,Cu_{1-x})Zr_2$. As shown in Fig. 3(a) and (b), the nanocrystals in the $Zr_{55}Cu_{30}Al_{10}Ni_5$ MG irradiated in this study have a distinctive bi-modal size distribution. One group has a nominal size range of 5–10 nm whereas the second has a range from 50 to 100 nm. While the chemical composition of the two different crystallite groups was not determined for this paper, it is unlikely that the large crystals contain a significant quantity of Ni, since it is a minority element in $Zr_{55}Cu_{30}Al_{10}Ni_5$ MG. Following this logic, it is possible to hypothesize that the larger crystal may be the $Cu_{10}Zr_7$ phase and the smaller crystals may be the $(Ni_x,Cu_{1-x})Zr_2$ phase, but a more detailed characterization is required to make this a definitive conclusion.

Even so, the most important point for the moment is that our study shows clear evidence that ion irradiation does indeed induce nanocrystal formations in $Zr_{55}Cu_{30}Al_{10}Ni_5$ glass. Metallic glasses are metastable at room temperature and crystallization occurs when energy is provided. Our results clearly demonstrate that ion irradiation can influence the crystallization process, which is governed by nucleation and crystal growth mechanisms that are enhanced by increasing atomic mobilities. During ion irradiation, displacement creation by energetic particles creates vacancy defects, which increases the free volume within the system, thus enhancing atomic mobility. In addition, the amount of energy loss of the particle will result in local heating, which also contributes to increased atomic mobility. Thus, ion irradiation will enhance chemical decomposition and periodic composition fluctuations and lead to nucleation site formation.

Our finding is in contrast to that by Nagata et al. [29], who reported that ion irradiation of the same alloy at room temperature did not cause any noticeable changes. In their studies, the Cu-ion energy was 350 keV and the ion fluence was $4 \times 10^{16}\,cm^{-2}$. In our study, the Cu-ion energy was 1 MeV and the ion fluence was $1 \times 10^{16}\,cm^{-2}$. According to a stopping and range of ions in matter (SRIM) calculation, the total displacements per ion for 350 keV Cu is 6.4×10^3 and for 1 MeV Cu, 1.4×10^4. Multiplied by ion fluencies, the total displacements for the previous and present studies are $2.6 \times 10^{20}\,cm^{-2}$ and $1.4 \times 10^{20}\,cm^{-2}$, correspondingly. Thus, the displacement creation is comparable in both studies. It is not clear to us why these two studies lead to opposite conclusions. However, it is important to point out that in the Nagata study, only X-ray diffraction was used to characterize the irradiated samples. Considering XRD's relatively high detection limits, determination of nanocrystalline phases could be difficult without further analysis using the TEM and SAD techniques employed in this study.

Introducing nanocrystals in MGs can enhance their ductility. But both crystal size and density must be optimized [1]. Although low temperature annealing can form bulk nano-crystalline alloys, this technique has difficulties for bulk MGs due to the large exothermic heat of crystallization generated inside the alloy [41]. In other words, using annealing to induce partial crystallization lacks controllability in bulk MGs. Ion irradiation can be used as a surface modification technique with high repeatability. Although the modification is limited by the ions' penetration depths, high energy light ion irradiation or electron irradiation can be used to alleviate these issues.

4. Summary

We investigated structural changes of $Zr_{55}Cu_{30}Al_{10}Ni_5$ metallic glass upon irradiation with 1 MeV Cu ions to a fluence of $1.0 \times 10^{16}\,cm^{-2}$. Post irradiation characterization using TEM reveals nanocrystal formation and SAD analysis suggests that the nanocrystalline phases are a mixture of $Cu_{10}Zr_7$, $NiZr_2$ and $CuZr_2$ phases with the possible formation of a substitutional intermetallic $(Ni_xCu_{1-x})Zr_2$ phase. In addition, the observed nanocrsytals have a distinctive bi-modal size distribution. Small nanocrystals with typical sizes ranging from 5 to 10 nm and large nanocrystals with typical sizes ranging from 50 to 100 nm are observed. These findings are different from a previous study which reported no structural changes upon ion irradiation of the same alloy.

Acknowledgements

This work was financially supported by the University Embryonic Technologies Program from Siemens Power Generation Emerging Technologies. L. Shao would like to acknowledge the support from the NRC Early Career Development Grant. X. Zhang acknowledges the support by DOE under grant number DE-FC07-05ID14657. This work was performed, in part, at the Center for Integrated Nanotechnologies, a DOE-supported user facility. The University of Houston group is supported from the State of Texas through Texas Center for Superconductivity at University of Houston, and through the DOE under Grant Number DE-FG02-05ER46208.

References

[1] A. Inoue, Acta Mater. 48 (2000) 279.
[2] A. Peker, W.L. Johnson, Appl. Phys. Lett. 63 (1993) 2342.
[3] W.L. Johnson, MRS Bull. 24 (1999) 42.
[4] M.F. Ashby, A.L. Greer, Scr. Mater. 54 (2006) 321.
[5] A.I. Salimon, Mater. Sci. Eng. A 375 (2004) 385.
[6] A.L. Greer, Science 267 (1995) 1947.
[7] A. Peker, W.L. Johnson, Appl. Phys. Lett. 63 (1993) 2343.
[8] X.Y. Jiang, Z.C. Zhong, A.L. Greer, Mater. Sci. Eng. A 789 (1997) 226.
[9] R. Schulz, M.L. Trudeau, D. Dussault, A. Van Neste, J. Phys. 51 (1990) C4259.
[10] H. Chen, Y. He, G.J. Shiflet, S.J. Poon, Nature 367 (1994) 6463.
[11] J.-J. Kim, Y. Choi, S. Suresh, A.S. Argon, Science 295 (2002) 654.
[12] J. Carter, E.G. Fu, G. Bassiri, B.M. Dvorak, N.D. Theodore, G.Q. Xie, D.A. Lucca, M. Martin, M. Hollander, X. Zhang, L. Shao, Nucl. Instr. and Meth. B 267 (2009) 1518.
[13] X.W. Du, M. Takeguchi, M. Tanaka, K. Furuya, Appl. Phys. Lett. 82 (2003) 1108.
[14] T. Nagase, Y. Umakoshi, Mater. Trans. 46 (2005) 616.
[15] J. Carter, E.G. Fu, M. Martin, G.Q. Xie, X. Zhang, Y.Q. Wang, D. Wijesundera, X.M. Wang, W.K. Chu, Lin Shao, Scripta Mater. 61 (2009) 265.
[16] G.Q. Xie, Q. Zhang, D.V. Louzguine-Luzgin, W. Zhang, A. Inoue, Mater. Trans. 47 (2006) 1930.
[17] A. Inoue, T. Zhang, Y.H. Kim, Mater. Trans. JIM 38 (1997) 749.
[18] L.Q. Xing, C. Bertrand, J.-P. Dallas, M. Cornet, Mater. Sci. Eng. A 241 (1998) 216.
[19] M.W. Chen, A. Inoue, C. Fan, A. Sakai, T. Sakurai, Appl. Phys. Lett. 74 (1999) 2131.
[20] T. Yamasaki, S. Maeda, Y. Yokoyama, D. Okai, T. Fukami, H.M. Kimura, A. Inoue, Intermetallics 14 (2006) 1102.
[21] A. Castellero, S. Bossuyt, M. Stoica, S. Deledda, J. Eckert, G.Z. Chen, D.J. Fray, A.L. Greer, Scr. Mater. 55 (2006) 87.
[22] J. Zhang, Y.H. Wei, K.Q. Qiu, H.F. Zhang, M.X. Quan, Z.Q. Hu, Mater. Sci. Eng. A 357 (2003) 386.
[23] F. Jiang, Z.J. Wang, Z.B. Zhang, J. Sun, Scr. Mater. 53 (2005) 487.
[24] M. Iqbal, J.I. Akhter, W.S. Sun, J.Z. Zhao, M. Ahmad, W. Wei, Z.Q. Hu, H.F. Zhang, Mater. Lett. 60 (2006) 662.
[25] N. Van Steenberge, A. Concustell, J. Sort, J. Das, N. Mattern, A. Gebert, S. Surnach, J. Eckert, M.D. Baró, Mater. Sci. Eng. A 491 (2008) 124.
[26] L. Liu, K.C. Chan, T. Zhang, J. Alloy Compd. 396 (2005) 114.
[27] E.G. Fu, J. Carter, M. Martin, G.Q. Xie, X. Zhang, Y.Q. Wang, R. Littleton, Lin Shao, Scripta Mater. 61 (2009) 40.
[28] M. Iqbal, J.I. Akhter, Z.Q. Hu, H.F. Zhang, A. Qayyum, W.S. Sun, J. Non-Cryst. Solids 353 (2007) 2452.
[29] S. Nagata, S. Higashi, B. Tsuchiya, K. Toh, T. Shikama, K. Takahiro, K. Ozaki, K. Kawatusra, S. Yamamoto, A. Inouye, Nucl. Instr. and Meth. B 257 (2007) 420.
[30] E.G. Fu, J. Carter, M. Martin, G.Q. Xie, X. Zhang, Y.Q. Wang, R. Littleton, Lin Shao, unpublished.
[31] The International Center for Diffraction Data, <http://www.icdd.com>.
[32] T. Nagase, Y. Umakoshi, J. Appl. Phys. 93 (2003) 912.
[33] N. Mattern, U. Kühn, H. Hermann, S. Roth, H. Vinzelberg, J. Eckert, Mater. Sci. Eng. A 375–377 (2004) 351.
[34] S.M. McDeavitt, D.P. Abraham, J.Y. Park, J. Nucl. Mater. 257 (1998) 21.
[35] D.P. Abraham, J.W. Richardson, S.M. McDeavitt, Mater. Sci. Eng. A 239 (1997) 658.
[36] J.L. Vrai, F.J. Humphreys, S.E. Burrows, J. Mater. Sci. 15 (1980) 1231.

[37] E.M. Carvalho, I.R. Harris, J. Mater. Sci. 15 (1980) 1224.
[38] Y.F. Sun, B.C. Wei, Y.R. Wang, W.H. Li, T.L. Cheung, C.H. Shek, Appl. Phys. Lett. 87 (2005) 051905.
[39] P. Garoche, J. Bigot, Phys. Rev. B 28 (1983) 6886.
[40] H.R. Wang, Y.F. Ye, Z.Q. Shi, X.Y. Teng, G.H. Min, J. Non-Cryst. Solids 311 (2002) 36.
[41] T.-S. Chin, C.Y. Lin, M.C. Lee, R.T. Huang, S.M. Huang, Mater. Today 12 (1&2) (2009) 34.